

Prebiotic Chemistry

Environmental History is Transferred via Minerals Altering Formose Reaction Pathways

Thijs J. de Jong, Astra D. Demertzi, William E. Robinson,* and Wilhelm T. S. Huck*

Abstract: It is generally accepted that minerals were an important source of prebiotic catalysis. In this work we demonstrate how the prebiotic sugar forming formose reaction is guided to unique reaction compositions in the presence of a variety of minerals. When the same mineral is transferred between multiple sequential batch reactions, a new reaction composition is obtained after each reaction cycle. We attribute this effect to the adsorption of catalytic $\text{Ca}(\text{OH})_2$ to mineral surfaces. Further exploration shows that first exposing the mineral surface to the aqueous catalyst allows the mineral to subsequently produce formose outputs without the need for any additional catalyst to be present. As such, the mineral surface functions as storage of the preceding environmental conditions. Our work supports the development of chemical complexity through the transfer of information between sequences of chemical environments.

Understanding how complex, life-supporting systems arose from the prebiotic environment remains a fundamental challenge. Chemists have made great strides toward finding plausible prebiotic synthetic routes toward the different molecular building blocks of life,^[1–4] and its metabolic cycles.^[5–7] These building blocks must have taken part in a process of chemical evolution to yield increasingly complex systems with emergent properties such as self-sustenance and self-replication.^[8] One of the key elements of chemical evolution is a sense of “history”. Information from previous event must have some impact on extant system states so that the system can adapt and learn from its environment. Within a chemical reaction network (CRN), acceleration of one or a few reactions can lead to significant reorganization of the network as a whole.^[9,10]

Our previous work on the formose reaction, a model prebiotic CRN, has shown that its outcomes are significantly shaped by modulating the concentration of the catalyst $\text{Ca}(\text{OH})_2$.^[11,12] The formose reaction generates a large number of sugars through the oligomerization of formaldehyde (FA) requiring only a simple initiating sugar such as dihydroxyacetone (DHA, **3**), a divalent metal ion catalyst such as Ca^{2+} , and alkaline conditions. Through a combination of four

reaction types, enolate formation, aldol additions, retro aldol reactions, and the Cannizzaro reaction a vast range of sugars are formed, including several potential autocatalytic cycles, such as the Breslow cycle (Figure 1a).^[13–16] Because of the high interconnectivity in the network, the formose reaction self-organizes in response to changes in its environment, such as catalyst concentration.^[11,12]

Minerals were ubiquitous in the prebiotic environment, and could have played a role in creating local microenvironments, concentrating chemical species, adsorbing and stabilizing molecules, and promoting a wide range of catalytic functions.^[17–23] Previous work has demonstrated that minerals change the outcome of the formose reaction at elevated temperatures and over extended time periods,^[24–29] or under dry conditions.^[26,30] Other research has concentrated on how various minerals stabilize formose intermediates, with a focus on obtaining biologically relevant sugars.^[31–33] Minerals have previously been shown to affect formose compositions in recursive cycle experiments, when part of the reaction mixture was retained between cycles.^[34]

In this work we explore the impact of different minerals on the formose reaction using high resolution GC(-MS) techniques,^[35] and demonstrate how minerals direct the compositional outcomes of the formose reaction. Furthermore, we demonstrate how reusing the same mineral between consecutive batch reactions affects the composition of subsequent formose reactions (Figure 1b,c). We discovered that the formose catalysts Ca^{2+} and NaOH , absorb to the surface of hydroxylapatite, goethite, and silicate minerals, thereby activating the surface to enable the production of formose products. These activated minerals were effective solid-supported catalysts for formose reactions lacking any other aqueous catalysts. Our findings support prebiotic scenarios where the catalytic effect of minerals is dynamically altered through sequences of reaction conditions, providing a potential mechanism for environmental information transfer supporting chemical evolution.

[*] T. J. de Jong, A. D. Demertzi, W. E. Robinson, W. T. S. Huck
Department of Physical Organic Chemistry, Institute for Molecules
and Materials (IMM), Radboud University, Nijmegen, Netherlands
E-mail: william.robinson@ru.nl
wilhelm.huck@ru.nl

Additional supporting information can be found online in the
Supporting Information section

© 2025 The Author(s). Angewandte Chemie International Edition
published by Wiley-VCH GmbH. This is an open access article under
the terms of the [Creative Commons Attribution-NonCommercial](#)
License, which permits use, distribution and reproduction in any
medium, provided the original work is properly cited and is not used
for commercial purposes.

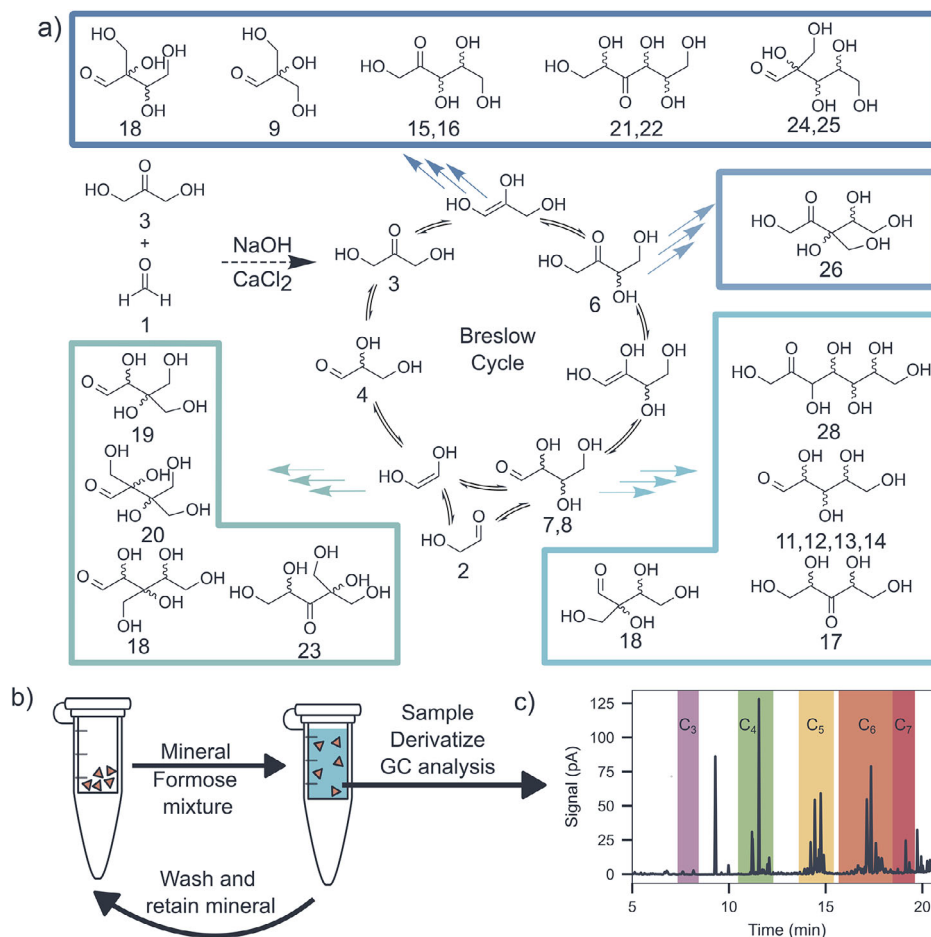


Figure 1. a) Schematic overview of formose reaction products, with the central autocatalytic Breslow cycle. b) General experimental procedure, a combination of different parts of the complete formose mixture (NaOH, CaCl₂, DHA, and FA) is added to powdered mineral. After the reaction period the mixture is sampled and analyzed using GC(-MS) after being derivatized. c) The rest of the supernatant is removed, and the mineral is washed and reused for subsequent reactions.

We selected nine different minerals native to the Hadean environment^[36] from different mineral classes: oxides (goethite, magnesium hydroxide, and titanium oxide); silicates, including iron silicate, zirconium silicate, and the phyllosilicates (kaolin, kaolinite, and montmorillonite); and a phosphate (hydroxylapatite) (for structures see Figures S2 and S3). To explore the impact of these minerals on the formose reaction, we performed reactions under a set of standardized formose reaction conditions ([NaOH] = 25 mM, [CaCl₂] = 10 mM, [DHA] = 35 mM, and [FA] = 50 mM) in the presence of nine different minerals. Expanding on previous work,^[34] we studied recursive batch reactions in which the formose reaction was performed in the presence of a mineral, which was then separated from the aqueous phase through centrifugation, washed and used for subsequent reaction cycles with fresh formose reaction mixture. Compound intensity is expressed as the gas chromatography (GC) peak height divided by the tetradecane internal standard (IS) used during analysis.

In the initial reaction cycle the effect of each mineral can be compared to the blank where no mineral was added (Figure 2a). The compositional outcomes for each mineral

were significantly different, as can be seen in the comparative bar plots in Figure 2a, and the principal component analysis (PCA) plot in Figure 2b. In general, the presence of minerals decreased the concentration of the Cannizzaro product (5), while increasing the amount of glyceraldehyde (4), erythrulose (6), and other tetroses. Previous work noted similar trends with increasing Ca²⁺ concentrations, which was attributed to inhibition of aldol addition reactions. In the presence of hydroxylapatite and montmorillonite, the amount of the branched C₄ 6, a direct product of DHA-FA addition, decreased. Most minerals caused an increase in branched C₅ sugars (19, 20) while selectively decreasing the amount of several aldopentoses (12–15). The amount of ketopentose 16 decreased (though not for hydroxylapatite) while the amount of ketopentose 17 increased. Simultaneously, branched C₆ compounds (21, 24–27) decreased, while for some of the minerals the amount of 3-ketohexoses (22, 23) increased.

To compare the compositional trajectories of each recursive reaction sequence, a PCA based dimensionality reduction of the composition from all reactions was performed (Figure 2b). Blank cycles, containing no mineral, are also

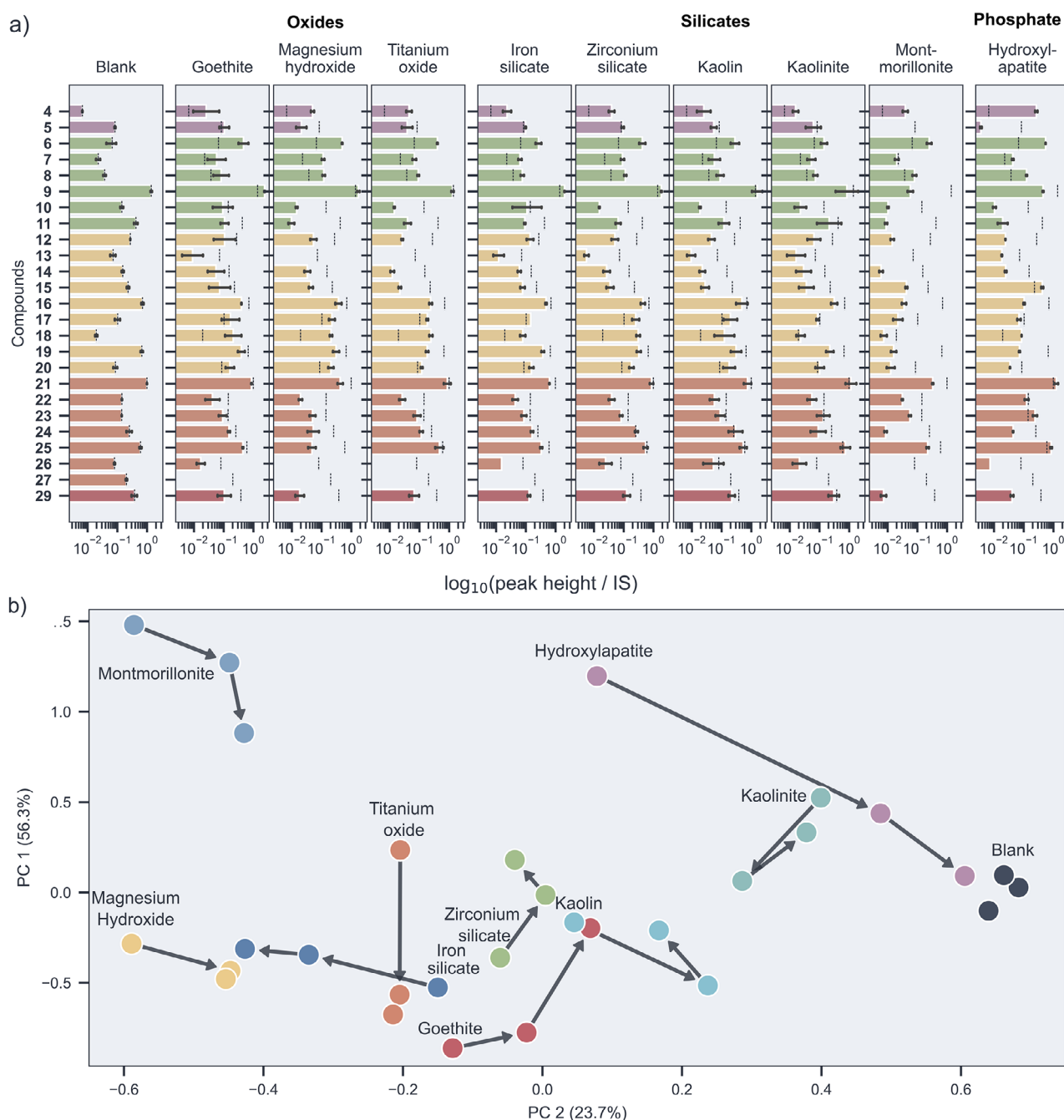


Figure 2. a) Log scale comparison of the formose reaction composition in the presence of various minerals showing trioses (purple), tetroses (green), pentoses (yellow), hexoses (orange), and heptoses (red). Dashed lines indicate the intensity of the compound in the blank sample. An overview of all structures is presented in Figure S1. b) Principal component analysis of the composition formed over three consecutive reactions, in the presence of various minerals. Arrows indicate washing steps, and show the order of compositions over the cycles. Oxides are colored in yellow, orange, and red, silicates are colored in shades of blue to green, and the phosphate in purple and the blank in black. The first two principal components are plotted, which account for 80.0% of variance. Bars and points are average values, and error bars denote one standard deviation, $n = 2,3$.

included in this plot. Interestingly, mineral identity has a clear effect on both the compositional outcome of the formose reaction, but also on how much the composition varies over a sequence of reaction steps. A detailed overview of compositions (including errors) is presented in Figures S4–S13. Figure 2b shows that for montmorillonite, hydroxylapatite, goethite, zirconium silicate, and iron silicate there is a clear evolution of the composition across different cycles. For

montmorillonite, the concentration of nearly all compounds increases with each cycle, indicating an overall increase of formose product formation over the reaction cycles. Zirconium silicate and goethite show increases in the production of aldopentoses, while there is a decrease in most tetroses, notably the branched C_4 9. Over the reaction cycles, goethite increases the concentration of various aldopentoses (12–15) and 3-ketohexoses (22, 23) while decreasing the branched

compounds **20**, **21**, **24**, and **25**. Hydroxylapatite shows the largest change between the first and second cycle, shifting aldopentose formation from **15** to **12**, and promoting the ketopentoses (**16**, **17**) and various branched sugars (**9**, **19**, **20**, **24**, and **26**). For zirconium silicate the detailed changes in the composition (Figure S13) show larger increase than is obvious from the PCA. Through the reaction cycles zirconium silicate promotes the formation of the various aldopentoses (**12–15**) and 3-ketohexoses (**22**, **23**), while decreasing the concentration of the branched compounds **9**, **21**, **24**, and **25**.

For magnesium hydroxide and titanium oxide, the largest compositional changes occur in the first two reaction cycles, whereas the third cycle exhibits little change in compositional outcome. Titanium oxide promotes the formation of **9** and a variety of C₅ compounds (**12**, **16–20**, and **24**). For magnesium hydroxide the overall changes are minor when inspecting the detailed composition and corresponding errors (Figure S11). For kaolin and kaolinite, the changes in composition appear to revert toward their first-cycle composition in Figure 2b. However, this can be attributed to the amplification of small changes during the PCA analysis, as the compositions appear similar, but with significant experimental error (Figures S9, S10).

Oxides exhibited the smallest changes in formose composition across cycles (Figure 2a), except for goethite, which behaves more similarly to zirconium silicate. Kaolin and kaolinite experiments showed a higher experimental error, suggesting the observed variations might not be significant, potentially due to lack of homogeneity in the mineral. Hydroxylapatite displays substantial changes across cycles, with the most significant change between the first two cycles.

These compositional changes indicated to us that the minerals were not only directing the formose reaction, but were also modified by the reaction mixtures. As a control experiment (with montmorillonite), we substituted the standardized formose condition with solutions of NaOH and CaCl₂ in the first two reaction cycles, followed by a third reaction cycle with the standardized formose reaction (Figure S14). The compositional outcome of the reaction is similar to the outcome for when the first two cycles are “standard” formose reaction conditions. These results demonstrate that the marked differences over the reaction cycles result not from a carry-over of small amounts of formose products, but instead we postulate this is caused by adsorption of the aqueous catalysts onto the mineral surface.

We investigated the role of adsorbed catalysts for a subset of the minerals (montmorillonite, hydroxylapatite, and magnesium hydroxide), chosen for behavior which are representative of previous experiments, where montmorillonite and hydroxylapatite showed a high degree of change over the consecutive reaction cycles, while magnesium hydroxide showed only a minor change in activity. These minerals were first incubated with either water or an aqueous solution of catalysts (CaCl₂ and NaOH), washed, and then incubated with FA and DHA (the formose reaction mixture *without* any catalyst). The sequence of water followed by FA and DHA demonstrates the native reaction directing effect of each mineral. Montmorillonite and magnesium hydroxide show very low activity, whereas hydroxylapatite shows significant

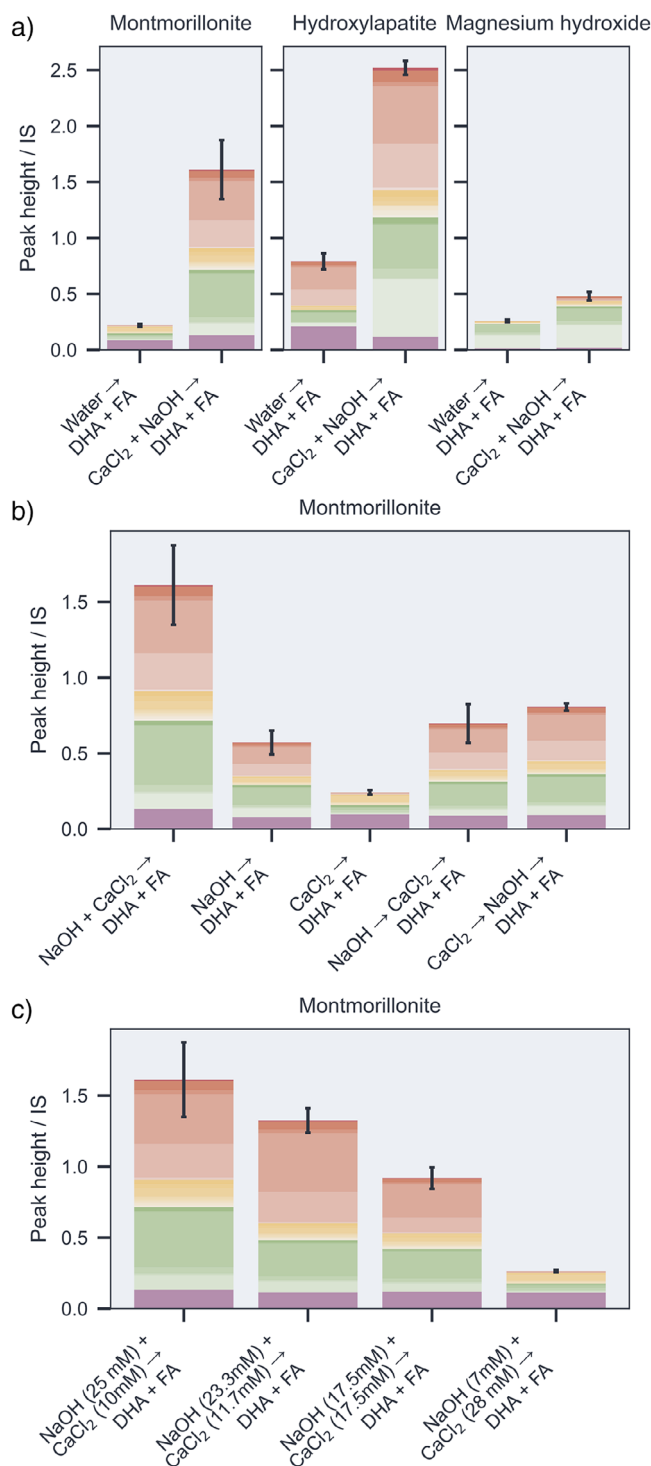


Figure 3. Stacked barplots showing how preceding environments influence the reaction outcomes produced by minerals. Showing trioses (shades of purple), tetroses (shades of green), pentoses (shades of yellow), hexoses (shades of orange), and heptoses (shades of red). Error bars indicate the total error according to $\sigma_{\text{total}} = \sqrt{\sum \sigma_i^2}$ where σ_i represents the error of individual species. Arrows in the tick labels denote separate cycles, and the last arrow also denotes a washing step. a) Comparison of formose products formed by different minerals that were first suspended in water or a solution of CaCl₂ and NaOH, followed by a cycle with DHA and FA. b) Study of the effect of individual aqueous catalyst components and their order of addition. Minerals are

build-up of formose reaction products (Figures 3a, S15, and S16). The latter is not surprising, considering the presence of Ca^{2+} and hydroxyl ions in hydroxylapatite. For hydroxylapatite the amount of C_6 compounds formed increased and the overall composition was enriched in C_4 compounds after incubation with NaOH and CaCl_2 . This indicates there is a shift from sugar-sugar addition to sugar-FA addition. For montmorillonite, the production of various compounds was promoted, mainly in the DHA-FA addition products erythrulose (**6**) and the branched tetrose **9** (Figure S17). In addition, formation of **21** and **26** was promoted. Comparing the three minerals, it is clear that both the native surface and the adsorbed catalysts may play a role in catalyzing the formose reaction. Even though we expected the hydroxide ions to play a role, magnesium hydroxide showed very little effect on the formose reaction composition.

Intrigued by this effect, we set out to explore the adsorption of CaCl_2 and NaOH in more detail, limiting the study to montmorillonite due to the more significant difference between its native and “activated” activity. We incubated montmorillonite with solutions of CaCl_2 or NaOH, before adding the incubated montmorillonite to a mixture of only DHA and FA. Comparatively, the combination of CaCl_2 and NaOH showed the largest increase in formation of formose products (Figure 3b). Sequential addition of the aqueous catalysts still demonstrated increased formation of formose products with the CaCl_2 followed by NaOH sequence showing a slightly increased activity compared to NaOH followed by CaCl_2 . Addition of only the individual catalysts resulted in much lower production of sugars. Notably, the addition of only CaCl_2 showed the lowest activity, comparable to the native catalytic activity of montmorillonite. These results indicate that both Ca^{2+} and hydroxide are transferred on mineral surfaces over reaction sequences. We hypothesize that NaOH activates the montmorillonite surface by deprotonating surface silicate groups, thus providing more binding sites for catalytic Ca^{2+} , and subsequently basic silicate groups increasing the pH of following reaction steps. Alternatively, amorphous calcium or sodium silicates could have been formed on the mineral surface. It has been well established that silicates in solution can catalyze the formose reaction.^[31]

Having established that pre-treating montmorillonite effectively provides a catalytically activated surface, we studied whether the ratio of CaCl_2 and NaOH used in the initial incubation (while keeping their total concentration constant), influenced the composition of the formose reaction (again, only FA and DHA were added). We systematically varied the NaOH: CaCl_2 ratios from 2.5:1 to 0.25:1. Figure 3c shows a clear decrease in formose reaction products as the amount of NaOH decreased. Our experiments reinforce the notion that NaOH activates the mineral surface. The stability

of the activated mineral surface was tested by performing up to six subsequent cycles with only DHA and FA (Figure S19). Although there is a steady decrease in total amount of product formed, after six cycles there is still a clear increase of catalytic activity compared to the native surface effect. Similarly, repeated washings with water before the addition of DHA and FA caused a slow decay in the activity of the mineral surface (Figure S22). Acidic conditions (pH 4) did not result in a substantial production of sugars (Figure S24). Increasing the ionic strength through addition of NaCl together with DHA and FA resulted in a small decrease of formose products (Figure S24). When the mineral surface was repeatedly incubated with low concentrations of NaOH (2.5 mM) and CaCl_2 (1 mM) there was a small increase in product formation as aqueous catalyst accumulated on the surface (Figure S26).

To conclude, we have demonstrated that various minerals affect the compositional outcomes of the formose reaction. These minerals retain information of their past environments, influencing subsequent reactions. This environmental history arises from the adsorption of Ca^{2+} and hydroxide onto the minerals' surfaces. This work focused on using Ca^{2+} as a catalyst as its catalytic effect on the formose reaction is well established. Future work could include studying other divalent metal ions, including Fe^{2+} , Mg^{2+} , or Sr^{2+} , which have been shown to affect the formose reaction.^[37] By acting as solid-supported catalysts, minerals allow reactions to occur in the absence of a solution source of catalysis, thus reducing the need for simultaneous presence of all reaction components. This relaxes the stringent requirements for prebiotic scenarios, allowing for the possibility of more flexible and dynamic mechanisms for chemical evolution. In this manner, minerals connect different chemical systems across various environments which contain incompatible chemistries or propagate small environmental changes over space and time.

Acknowledgements

This work was funded by European Union and the Swiss State Secretariat for Education, Research and Innovation (SERI) under contract numbers 22.00017 and 22.00034 (Horizon Europe Research and Innovation Project CORENET), the Simons Collaboration on the Origins of Life (SCOL; award 477123), and the Onassis Foundation – Scholarship ID: F ZS 013–1/2022–2023. The authors thank Dr. P. Tinnemans for support with PXRD analysis.

Conflict of Interests

The authors declare no conflict of interest.

Data Availability Statement

The data that support the findings of this study are available in the supplementary material of this article.

Keywords: Aldehydes • Aldol reaction • Formose reaction • Minerals • Prebiotic chemistry

suspended in the shown (sequence) of solution of CaCl_2 and/or NaOH followed by a cycle with DHA and FA. c) Effect of different ratios of catalyst, minerals are first suspended in a solution with the reported concentrations of CaCl_2 and NaOH, followed by a cycle with DHA and FA. Experiments were performed in triplicate or duplicate, and bars are averages of the measurements.

- [1] B. H. Patel, C. Percivalle, D. J. Ritson, C. D. Duffy, J. D. Sutherland, *Nat. Chem.* **2015**, *7*, 301–307.
- [2] J. D. Sutherland, *Nat. Rev. Chem.* **2017**, *1*, 0012.
- [3] M. W. Powner, B. Gerland, J. D. Sutherland, *Nature* **2009**, *459*, 239–242.
- [4] S. Becker, J. Feldmann, S. Wiedemann, H. Okamura, C. Schneider, K. Iwan, A. Crisp, M. Rossa, T. Amatov, T. Carell, *Science* **2019**, *366*, 76–82.
- [5] K. B. Muchowska, S. J. Varma, J. Moran, *Chem. Rev.* **2020**, *120*, 7708–7744.
- [6] M. A. Keller, A. Zylstra, C. Castro, A. V. Turchyn, J. L. Griffin, M. Ralser, *Sci. Adv.* **2016**, *2*, e1501235.
- [7] R. Braakman, E. Smith, *Phys. Biol.* **2013**, *10*, 011001.
- [8] R. Krishnamurthy, N. V. Hud, *Chem. Rev.* **2020**, *120*, 4613–4615.
- [9] J. M. Horowitz, J. L. England, *Proc. Natl. Acad. Sci. USA* **2017**, *114*, 7565–7570.
- [10] Q. P. Tran, Z. R. Adam, A. C. Fahrenbach, *Life* **2020**, *10*, 352.
- [11] W. E. Robinson, E. Daines, P. van Duppen, T. de Jong, W. T. S. Huck, *Nat. Chem.* **2022**, *14*, 623–631.
- [12] P. Van Duppen, E. Daines, W. E. Robinson, W. T. S. Huck, *J. Am. Chem. Soc.* **2023**, *145*, 7559–7568.
- [13] I. V. Delidovich, A. N. Simonov, O. P. Taran, V. N. Parmon, *ChemSusChem* **2014**, *7*, 1833–1846.
- [14] C. Appayee, R. Breslow, *J. Am. Chem. Soc.* **2014**, *136*, 3720–3723.
- [15] R. Breslow, *Tetrahedron Lett.* **1959**, *1*, 22–26.
- [16] G. Harsch, M. Harsch, H. Bauer, W. Voelter, *Z. Naturforsch. B.* **1983**, *38*, 1269–1280.
- [17] A. V. Dass, K. Hickman-Lewis, A. Brack, T. P. Kee, F. Westall, *ChemistrySelect* **2016**, *1*, 4906–4926.
- [18] A. J. Surman, M. Rodriguez-Garcia, Y. M. Abul-Haija, G. J. T. Cooper, P. S. Gromski, R. Turk-MacLeod, M. Mullin, C. Mathis, S. I. Walker, L. Cronin, *Proc. Natl. Acad. Sci.* **2019**, *116*, 5387–5392.
- [19] S. Asche, R. W. Pow, H. M. Mehr, G. J. T. Cooper, A. Sharma, L. Cronin, *ChemSystemsChem* **2024**, *6*, e202400006.
- [20] B. Burcar, A. Castañeda, J. Lago, M. Daniel, M. A. Pasek, N. V. Hud, T. M. Orlando, C. Menor-Salván, *Angew. Chem.* **2019**, *131*, 17137–17143.
- [21] H. James Cleaves, II, A. Michalkova Scott, F. C. Hill, J. Leszczynski, N. Sahai, R. Hazen, *Chem. Soc. Rev.* **2012**, *41*, 5502–5525.
- [22] L. Vincent, M. Berg, M. Krismer, S. T. Saghafi, J. Cosby, T. Sankari, K. Vetsigian, H. J. Cleaves, D. A. Baum, *Life* **2019**, *9*, 80.
- [23] A. Z. Khalifa, Ö. Cizer, Y. Pontikes, A. Heath, P. Patureau, S. A. Bernal, A. T. M. Marsh, *Cem. Concr. Res.* **2020**, *132*, 106050.
- [24] A. G. Cairns-Smith, P. Ingram, G. L. Walker, *J. Theor. Biol.* **1972**, *35*, 601–604.
- [25] A. W. Schwartz, R. M. de Graaf, *J. Mol. Evol.* **1993**, *36*, 101–106.
- [26] S. Lamour, S. Pallmann, M. Haas, O. Trapp, *Life* **2019**, *9*, 52.
- [27] V. Vinogradoff, V. Leyva, E. Mates-Torres, R. Pepino, G. Danger, A. Rimola, L. Cazals, C. Serra, R. Pascal, C. Meinert, *Earth Planet. Sci. Lett.* **2024**, *626*, 118558.
- [28] S. Pallmann, J. Šteflová née Svobodová, M. Haas, S. Lamour, A. Henß, O. Trapp, *New J. Phys.* **2018**, *20*, 055003.
- [29] K. Usami, A. Okamoto, *Org. Biomol. Chem.* **2017**, *15*, 8888–8893.
- [30] M. Haas, S. Lamour, S. B. Christ, O. Trapp, *Commun. Chem.* **2020**, *3*, 140.
- [31] J. B. Lambert, S. A. Gurusamy-Thangavelu, K. Ma, *Science* **2010**, *327*, 984–986.
- [32] H. J. Kim, A. Ricardo, H. I. Illangkoon, M. J. Kim, M. A. Carrigan, F. Frye, S. A. Benner, *J. Am. Chem. Soc.* **2011**, *133*, 9457–9468.
- [33] S. Nitta, Y. Furukawa, T. Kakegawa, *Orig. Life Evol. Biospheres* **2016**, *46*, 189–202.
- [34] S. Colón-Santos, G. J. T. Cooper, L. Cronin, *ChemSystemsChem* **2019**, *1*, e1900014.
- [35] M. Haas, S. Lamour, O. Trapp, *J. Chromatogr. A* **2018**, *1568*, 160–167.
- [36] R. M. Hazen, *Am. J. Sci.* **2013**, *313*, 807–843.
- [37] Y. Shigemasa, T. Tajiri, E. Waki, R. Nakashima, *Bull. Chem. Soc. Jpn.* **1981**, *54*, 1403–1409.

Manuscript received: February 26, 2025

Revised manuscript received: March 20, 2025

Accepted manuscript online: March 20, 2025

Version of record online: March 27, 2025